PHYSICAL REVIEW A VOLUME 49, NUMBER 3 MARCH 1994

Interaction of half-cycle radiation pulse with Rydberg states of atomic hydrogen

K. J. LaGattuta and P. B. Lerner
Los Alamos National Laboratory, Los Alamos, New Mexico 87545
(Received 13 September 1993)

We describe the results of our solutions of the time-dependent Schrödinger equation for Rydberg states of atomic hydrogen exposed to a short pulse of "half-cycle" long-wavelength radiation. By "short" we mean that the duration of the pulse is much less than the Kepler period of the Rydberg state being irradiated. Comparison is made with the results of experiments which have been reported recently [R. Jones, D. You, and P. Bucksbaum, Phys. Rev. Lett. **70**, 1236 (1993)].

PACS number(s): 32.80.Rm

INTRODUCTION

We report here the results of our simulations of the interaction of a pulse of long-wavelength, single-polarity radiation with the Rydberg states of atomic hydrogen. The time-dependent Schrödinger equation (TDSE) was invoked, and its solution was obtained by a standard numerical method [1].

Experiments conducted by Jones, You, and Bucksbaum [2] have revealed an interesting variation of the ionization fraction P_{ioniz} of excited Na atoms with the principal quantum number of the initially occupied Rydberg state n_i, provided that the pulse length is much less than the Kepler period; i.e., if $t_{\text{pulse}} \ll 2\pi n_i^3$. In this case, they observed that the peak electric field strength E_0 needed to produce a fixed ionization fraction varied according to $E_0 \propto 1/n_i^2$, for $P_{\text{ioniz}} \sim 0.1$. For $P_{\text{ioniz}} \sim 0.5$, the observed scaling changed to $E_0 \propto 1/n_i^{1.5}$. This is in contrast to the well-known behavior in the "long pulse" limit [3], where $E_0 \propto 1/n_i^4$.

We have verified these results by means of our simulations conducted on hydrogen, a similar system. However, we found that the scaling reported in Ref. [2] is fortuitous, and is a special case of a more general behavior. This has been pointed out already by others [4].

In addition, we computed spectra of emitted electron kinetic energies e_c. At relatively high values of the peak electric field strength E_0, these were quasiexponential functions of e_c, with a decay constant which depended on the value of E_0. There was a simple relationship between this decay constant and the spatial extent of the escaping electron wave packet.

In order to facilitate the numerical calculation, we scaled down both the pulse length and the range of n_i values considered in Ref. [2]. We have focused our attention on the Rydberg states for which $4 \le n_i \le 9$, and taken a pulse length $t_{\text{pulse}} = 54\pi$ a.u. $= 4$ fsec. This t_{pulse} corresponds to the Kepler period of an electron with principal quantum number $n = 3$. Here, and in the following, all quantities are in atomic units (a.u.).

FORMALISM

More precisely, we considered a "half-cycle" pulse of the form

$$\mathbf{E}(t) = -\hat{\mathbf{z}} E_0 \sin^2(t/54) \tag{1}$$

for $0 \le t \le 54\pi$ a.u., and solved the TSDE

$$\left[-\tfrac{1}{2}\nabla^2 - 1/r + \mathbf{r}\cdot\mathbf{E}(t) - \frac{i\partial}{\partial t} \right] \Psi(\mathbf{r},t) = 0 \tag{2}$$

subject to the initial condition

$$\Psi(\mathbf{r},0) = \Phi_i(\mathbf{r}) , \tag{3}$$

where Φ_i is the initial Rydberg state of hydrogen, and i denotes $n_i l_i m_i$. The wave function $\Psi(\mathbf{r},t)$ was expanded in partial waves, and Eq. (2) was solved numerically by a finite-difference method, on a radial mesh of size $\Delta r = 0.5$ a.u. A complete description of this approach is contained in Ref. [1].

The spectral power density of the driving field $S(\omega)$ [square of the Fourier transform of Eq. (1)] has a maximum at $\omega = 0$, and a half maximum for $\omega = 0.027$ a.u. For $\omega \gg 2\pi/t_{\text{pulse}}$, $S(\omega)$ falls as $1/\omega^6$; e.g., $S(\frac{1}{2})/S(0) = 10^{-8}$.

The emitted electron kinetic energy spectrum was obtained by projecting $\Psi(\mathbf{r},t)$, for $t = t_{\text{pulse}}$, onto Coulomb continuum functions Φ_c; i.e.,

$$dP_c/d\epsilon_c = \sum_{l_c} \left| \int d\mathbf{r}\, \Psi^*(\mathbf{r},t_{\text{pulse}}) \Phi_c(\mathbf{r}) \right|^2 , \tag{4}$$

where the continua are labeled by angular momentum l_c and energy ϵ_c. Since the pulse was linearly polarized, the azimuthal quantum number was a constant of the motion; $m_c = m_i$. The sum over continuum partial waves extended over the range $0 \le l_c \le (l_c)_{\max}$, where the requisite value of $(l_c)_{\max}$ depended on E_0. The ionization fraction was then

$$P_{\text{ioniz}} = \int d\epsilon_c \, dP_c/d\epsilon_c \ . \tag{5}$$

If the peak electric field strength E_0 were small enough, then the ionization fraction could be obtained from the first Born approximation (FBA) according to

$$P_{\text{ioniz}} \approx P_{\text{ioniz}}^{(\text{FBA})} = \sum_{l_c} \int d\epsilon_c \frac{|\langle c|\mathbf{E}_0\cdot\mathbf{r}|i\rangle|^2\Omega^4}{\epsilon_{ci}^2(\epsilon_{ci}^2-\Omega^2)^2} \times \sin^2(\epsilon_{ci}t_{\text{pulse}}/2) \quad (6)$$

for the pulse given by Eq. (1), where $\epsilon_{ci}=\epsilon_c-\epsilon_i$ is the difference in energy between the initial Rydberg and final continuum states, and $\Omega=2\pi/t_{\text{pulse}}$. Here, the sum over l_c was restricted by the dipole selection rule to $l_c=l_i\pm1$. Empirically, we found that the FBA was a good approximation, provided that $P_{\text{ioniz}}<0.001$ for $n_i\geq4$.

Excitation to other states within the bound manifold also occurred, and the probability for these transitions was obtained in analogy to Eqs. (4) and (5) as

$$P_f=\left|\int d\mathbf{r}\,\Psi^*(\mathbf{r},t_{\text{pulse}})\Phi_f(\mathbf{r})\right|^2, \quad (7)$$

where f labels the discrete Coulomb state with quantum numbers $n_f l_f$, and $m_f=m_i$.

It was also useful to consider the total energy gained by the electron during the pulse, according to

$$\Delta U_{\text{tot}}=\int d\epsilon_c\epsilon_c dP_c/d\epsilon_c+\sum_f \epsilon_f P_f-\epsilon_i \quad (8)$$

and the average displacement of the electron along the field direction, defined as

$$z_{\text{ave}}=\int d\mathbf{r}(\mathbf{r}\cdot\hat{\mathbf{z}})|\Psi(\mathbf{r},t_{\text{pulse}})|^2 . \quad (9)$$

RESULTS

For $P_{\text{ioniz}}<10^{-4}$, the FBA for the ionization fraction [Eq. (6)] could be applied successfully. For fixed l_i, this was parametrized as

$$P_{\text{ioniz}}^{(\text{FBA})}=AE_0^{\beta}n_i^{\alpha} \quad (10)$$

for constant A, where $\beta=2$, and $\alpha=\alpha(n_i)$ was an n_i-dependent exponent. For the pulse parameters described in the Introduction, and for $l_i=0$, we found that α varied smoothly over the range $6.3\geq\alpha\geq1.7$, as n_i varied from 4 to 15; see Fig. 1. Consequently, for fixed ionization fraction, the critical electric-field strength satisfied a relationship of the form $E_0\propto1/n_i^{\delta}$, for $\delta\equiv\alpha/2$, where $3.1\geq\delta\geq0.8$. Fortuitously, for $n_i=5$ or 6, we found that $E_0\propto1/n_i^{2.0}$.

For larger values of P_{ioniz}, the FBA underestimated the ionization probability, as judged by the full solution of the TDSE [Eq. (2)]; i.e., until P_{ioniz} approached 1.0. The results of solving Eq. (2), for $l_i=0$ and $3\leq n_i\leq9$, and then computing the ionization fraction from Eq. (5) appear in Fig. 2 for an extended range of E_0 values.

A cursory inspection of Fig. 2 shows that Eq. (10) fails for $P_{\text{ioniz}}>10^{-4}$, unless $\beta=\beta(E_0)$ is a function of E_0. A close inspection of the numerical data suggests that β is both a strong function of E_0 and a weak function of n_i, so that P_{ioniz} can be only approximately expressed as the product of a function of E_0 times a function of n_i.

However, for an arbitrary fixed value of P_{ioniz}, the electric field strength E_0 is still only a function of n_i (and l_i). In Fig. 3, we plot values of $E_0\equiv E_0(1\%)$ vs n_i, for $P_{\text{ioniz}}=0.01$ and $l_i=0$ (filled circles). Straight-line segments denote $E_0\propto1/n_i^{\delta}$ for $\delta=2$ (dotted) and $\delta=1$ (dashed). Over the range $3\leq n_i\leq9$, δ is seen to vary smoothly from ~2 to ~1. The range of n_i values over which $\delta\sim2$ is $3\leq n_i\leq5$. The values assumed by δ decrease slowly as P_{ioniz} increases. We also plot values of $E_0\equiv E_0(10\%)$ vs n_i for $P_{\text{ioniz}}=0.10$ (open circles). Now $\delta\sim1.5$ over the range $3\leq n_i\leq5$.

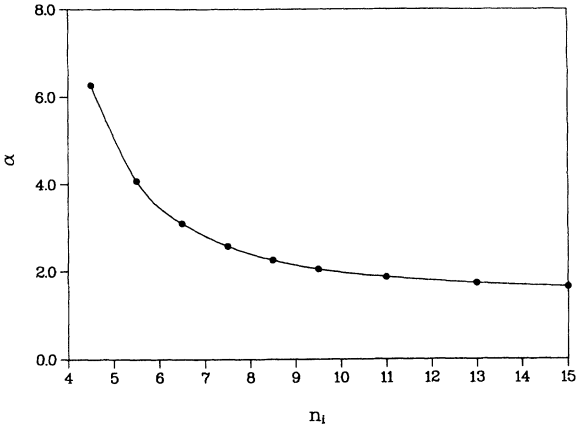

FIG. 1. Plot of α vs n_i for $P_{\text{ioniz}}<0.001$ from the FBA [Eq. (10)]. A spline fit to the data points has been added to guide the eye.

This behavior of δ is in fair agreement with the experiment [2], if our results are scaled to longer pulse length. In the experiment, the range of n_i values over which $\delta=2.0(1.5)$ was $15<n_i\leq30$, for 10% (50%) ionization. This can be rewritten as

$$n_{\text{Kepler}}<n_i\leq2n_{\text{Kepler}} , \quad (11)$$

where the pulse length is $t_{\text{pulse}}=2\pi n_{\text{Kepler}}^3$, and $n_{\text{Kepler}}\approx15$. We have also found that $\delta=2.0$ (1.5) over the range described by Eq. (11), but for $n_{\text{Kepler}}=3$ and for 1% (10%) ionization.

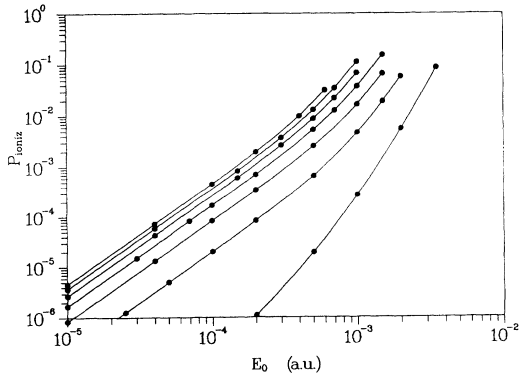

FIG. 2. Plot of P_{ioniz} vs E_0, for $l_i=0$ and $3\leq n_i\leq9$; results from the TDSE [Eq. (2) and (5)]. Data points are connected by spline fit, and appear consecutively from right ($n_i=3$) to left ($n_i=9$).

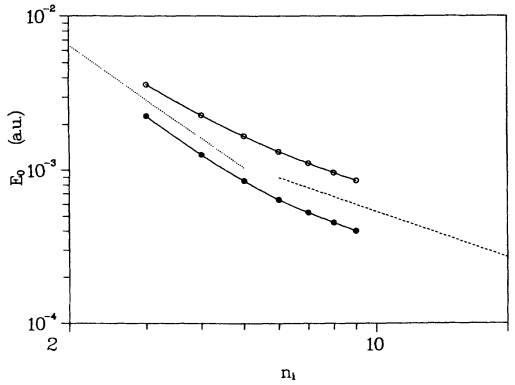

FIG. 3. Plot of $E_0(1\%)$ vs n_i, for $l_i=0$ (filled circles), and E_0 (10%) vs n_i for $l_i=0$ (open circles). Straight-line segments suggest behavior for $\delta=1$ (dashed), and $\delta=2$ (dotted).

The behavior of P_{ioniz} as a function of l_i was also investigated. In Fig. 4 we plot values of P_{ioniz} vs. E_0 for $n_i=6$ and $0\le l_i\le 5$; all for $m_i=0$. As expected, for E_0 small enough, we found that P_{ioniz} decreased as l_i increased, except for an initial small increase as l_i changed from 0 to 1. However, for $E_0>0.001$, the reverse was found to occur. That is, P_{ioniz} increased uniformly as l_i increased. We ascribe this behavior to the electric-field-induced mixing of the largest l_i values in the $n_i=6$ manifold with the smallest l_i values in the $n_i=7$ manifold. For initial states with $m_i=l_i$ this behavior was not observed.

Emitted electron kinetic energy spectra were obtained from Eq. (4), for fixed continuum angular momentum l_c, and also summed over all l_c. Generally, plots of $dP_c/d\epsilon_c$ vs ϵ_c, for fixed l_c, were highly structured, with numerous maxima and minima appearing in the range $0.0\le\epsilon_c\le 0.1$ a.u. (For larger energies, where $dP_c/d\epsilon_c$ was extremely small, numerical error intruded.)

However, spectra summed over l_c were smooth and of the form $dP_c/d\epsilon_c \propto \exp(-\sigma\epsilon_c)$, where σ was roughly independent of n_i and a weakly decreasing function of E_0 but a linearly increasing function of l_i. Setting $\epsilon_c=k_c^2/2$, this exponential distribution of continuum energies implied an approximately Gaussian form for the outgoing electron wave packet; i.e., $\exp(-\sigma k_c^2/2)\Longleftrightarrow\exp[-(z-z_p)^2/2\sigma]$, where $\Longleftrightarrow$ denotes a Fourier-transform pair, and the position of the center of the packet is z_p at $t=t_{\text{pulse}}$. The full width of the outgoing wave packet was then approximately $\Delta_z=2\sqrt{2\sigma}$. In Fig. 5 we plot a typical spectrum, for $n_il_i=6h$ $(m_i=0)$, at $E_0=0.001$ a.u. The corresponding outgoing wave packet (continuum probability density vs z) appears in Fig. 6. From Fig. 5 we estimated that $\sigma\sim 196$ a.u., so that $2\sqrt{2\sigma}\sim 40$ a.u. By comparison, from Fig. 6 we estimated that the full width (at $1/e$) of the outgoing wave packet was approximately 38 a.u.

It was also observed that the outcomes of these numerical calculations could be well represented, in their average behaviors, by completely classical calculations. For

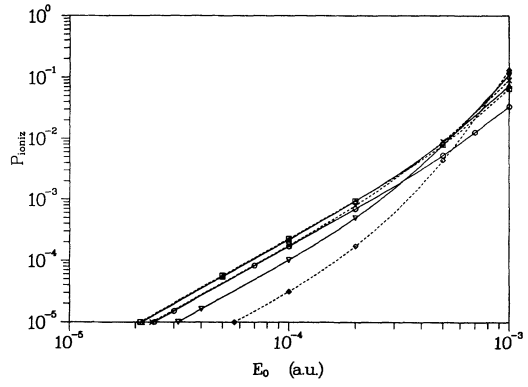

FIG. 4. Plot of P_{ioniz} vs E_0 for $n_i=6$ and $0\le l_i\le 5$ $(m_i=0)$; results are from the TDSE. Points for even (odd) angular momenta are connected by solid (dashed) spline fitted curves; $l_i=0$ (circle), $l_i=1$ (square), $l_i=2$ (triangle), $l_i=3$ (cross), $l_i=4$ (inverted triangle), $l_i=5$ (diamond).

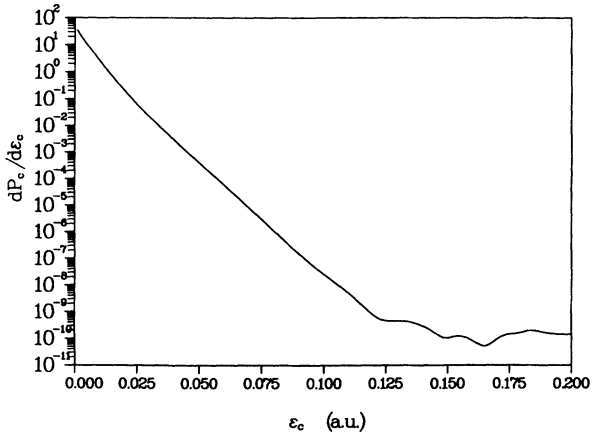

FIG. 5. Plot of $dP_c/d\epsilon_c$ vs ϵ_c, for $n_il_i=6h$ $(m_i=0)$ at $E_0=0.001$ a.u.; results are from the TDSE [Eqs. (2) and (4)]. Values for 0.025 a.u. $\le\epsilon_c\le 0.10$ a.u. follow the exponential curve; values for $\epsilon_c>0.10$ a.u. are due to numerical error; values for $\epsilon_c<0.025$ a.u. follow a power law.

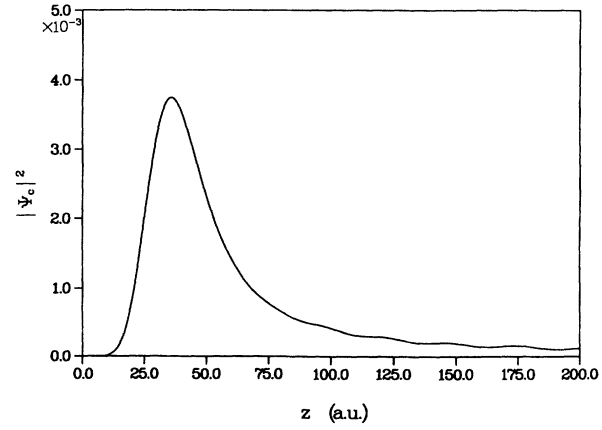

FIG. 6. Plot of $|\Psi_c|^2$ vs r, for the conditions of Fig. 4; results are from the TDSE [Eq. (2)]. This is the continuum portion of the probability density only, as computed at $t=t_{\text{pulse}}$.

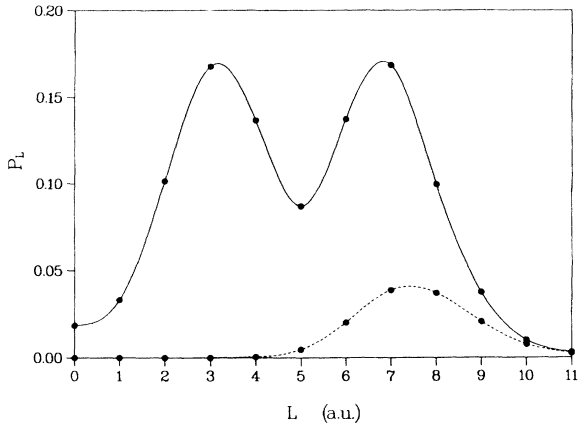

FIG. 7. Plot of the total probability in each partial wave, for the conditions of Fig. 4; results come from the TDSE. Points for bound plus continuum (continuum alone) are connected by solid (dashed) spline fitted curves.

instance, the average energy absorbed by the electron during the pulse could be obtained classically as $\Delta U_{\text{class}} = \frac{1}{8}(E_0 t_{\text{pulse}})^2$ from the so-called "simpleman's model" (SM) [5]. The SM also predicted the net electron displacement along the field direction to be $z_{\text{class}} = \frac{1}{4} E_0 t_{\text{pulse}}^2$. Not too surprisingly, both of these predictions were rather accurate for the larger n_i values, and especially for the larger l_i values, as judged by comparisons with the "exact" results obtained from Eq. (8) and (9).

It is interesting to note that, in those cases for which $P_{\text{ioniz}} < 0.1$, the amount of excitation to highly-lying Rydberg states was always found to be much greater than the amount of ionization; see Fig. 7. Nevertheless, both ΔU_{class} and z_{class} agreed well with the TSDE results. Evidently, for the purposes of applying the classical approximation, it was immaterial whether the electron was promoted into the continuum or into a higher-lying bound level.

Finally, we point out that, as for the continuum spectra, the probability of promotion into high-lying Rydberg states was a structured function of n_f, for fixed l_f, with numerous maxima and minima. Although, for $P_{\text{ioniz}} < 0.1$, the range of partial waves that were significantly populated grew only slowly with applied field strength (approximately as E_0^2); for $P_{\text{ioniz}} > 0.1$ there was a veritable "explosion" of probability into very high partial waves ($l_c \gg 10$). Presumably, some of these features are accessible to experimental examination. Their further elucidation through numerical work is already underway here.

SUMMARY

In this Rapid Communication we have described our numerical simulations of experiments [2] involving the interactions of Rydberg states with single-polarity, short-pulse radiation. We "scaled" the experimental conditions to shorter pulse length and lower n_i values, in order to facilitate these calculations.

We observed that the value of the peak electric-field strength needed to produce a given ionization fraction varied as an inverse power of n_i; i.e., as $E_0 \propto 1/n_i^{\delta}$. However, δ was found to depend on n_i, and its range of values was rather broad: $3 \geq \delta \geq 1$. This agreed with the predictions of Ref. [4]. The range of n_i values for which $E_0 \propto 1/n_i^2$ was found to be restricted to $n_{\text{Kepler}} < n_i \leq 2n_{\text{Kepler}}$, as it was in the experiment [2].

We also obtained spectra of emitted electron kinetic energies, and pointed out an interesting correlation between the shape of these spectra and the spatial width of the outgoing electron wave packet. Finally, completely classical calculations were applied to the determination of changes in electronic properties, which were then equated to quantum-mechanical expectation values. These classical calculations did not distinguish between high-lying bound and continuum electronic states, although TDSE results showed that the corresponding subspaces were both populated to a significant degree.

[1] K. La Gattuta, J. Opt. Soc. Am. B 7, 639 (1990).

[2] R. Jones, D. You, and P. Bucksbaum, Phys. Rev. Lett. **70**, 1236 (1993).

[3] H. Bethe and E. Salpeter, in *Quantum Mechanics of One and Two-electron Atoms* (Springer-Verlag, Berlin, 1957), p. 237.

[4] C. Reinhold, M. Melles, and J. Burgdorfer, Phys. Rev. Lett. **70**, 4026 (1993).

[5] P. Corkum, P. Burnett, and F. Brunel, Phys. Rev. Lett. **62**, 1259 (1989).